

UCSF

UC San Francisco Previously Published Works

Title

Adaptive deep brain stimulation for Parkinson's disease using motor cortex sensing.

Permalink

<https://escholarship.org/uc/item/5sp2f3rg>

Journal

Journal of neural engineering, 15(4)

ISSN

1741-2560

Authors

Swann, Nicole C
de Hemptinne, Coralie
Thompson, Margaret C
[et al.](#)

Publication Date

2018-08-01

DOI

10.1088/1741-2552/aabc9b

Peer reviewed



Published in final edited form as:

J Neural Eng. 2018 August ; 15(4): 046006. doi:10.1088/1741-2552/aabc9b.

Adaptive deep brain stimulation for Parkinson's disease using motor cortex sensing

Nicole C. Swann, Ph.D.^{*1,2}, Coralie de Hemptinne, Ph.D.¹, Margaret C. Thompson, M.A.³, Svtjetlana Miocinovic, M.D. Ph.D.⁴, Andrew M. Miller, B.S.¹, Ro'ee Gilron, Ph.D.¹, Jill L. Ostrem, M.D.⁵, Howard J. Chizeck, Ph.D.^{3,6}, and Philip A. Starr, M.D. Ph.D.¹

¹Department of Neurological Surgery, University of California, San Francisco

²Department of Human Physiology, University of Oregon

³Department of Electrical Engineering, University of Washington

⁴Department of Neurology, Emory University

⁵Department of Neurology, University of California, San Francisco

⁶Department of Bioengineering, University of Washington

Abstract

Objective—Contemporary deep brain stimulation for Parkinson's disease is delivered continuously, and adjustments based on patient's changing symptoms must be made manually by a trained clinician. Patients may be subjected to energy intensive settings at times when they are not needed, possibly resulting in stimulation-induced adverse effects, such as dyskinesia. One solution is “adaptive” DBS, in which stimulation is modified in real time based on neural signals that co-vary with the severity of motor signs or of stimulation-induced adverse effects.

Here we show the feasibility of adaptive DBS using a fully implanted neural prosthesis.

Approach—We demonstrate adaptive deep brain stimulation in two patients with Parkinson's disease using a fully implanted neural prosthesis that is enabled to utilize brain sensing to control stimulation amplitude (Activa PC+S). We used a cortical narrowband gamma (60-90 Hz) oscillation related to dyskinesia to decrease stimulation voltage when gamma oscillatory activity is high (indicating dyskinesia) and increase stimulation voltage when it is low.

Main Results—We demonstrate the feasibility of “adaptive deep brain stimulation” in two patients with Parkinson's disease. In short term in-clinic testing, energy savings were substantial (38-45%), and therapeutic efficacy was maintained.

Significance—This is the first demonstration of adaptive DBS in Parkinson's disease using a fully implanted device and neural sensing. Our approach is distinct from other strategies utilizing basal ganglia signals for feedback control.

*Corresponding author: Nicole C. Swann, PhD, Department of Human Physiology, University of Oregon, 122 Esslinger Hall, 1240 University of Oregon, Eugene, OR 97403, 458-205-5293.

Disclosures

UCSF has filed a preliminary patent related to this work and Drs. NCS, CD, JLO, and PAS are co-inventors on this patent.

Introduction

Deep brain stimulation (DBS) can be an effective treatment for Parkinson's disease (PD), but has limitations that reduce efficacy for individual patients and create barriers to more widespread application of the technique. Programming requires a trained clinician, can be time consuming and, for some patients, satisfactory settings are never achieved. Adverse effects related to therapy, such as dyskinesia, can occur in response to DBS. Since its introduction 25 years ago, DBS for PD has been delivered in a constant or "open-loop" manner without real-time adjustments based on patient's changing signs and symptoms. DBS could be improved by automated adjustment of stimulation in response to neural signatures of motor impairment or of stimulation-induced adverse effects. One approach, demonstrated using temporarily externalized DBS leads, utilized the amplitude of beta frequency oscillations in the subthalamic nucleus (STN) local field potential (LFP) to control the amplitude of STN stimulation^{1,2}. This "adaptive DBS" approach is promising but may be challenging to implement in fully implantable systems due to the small amplitude of the STN LFP coupled with the large stimulation artifact generated when sensing a signal in close proximity to the stimulating contact. Additionally, the challenges of stimulating and recording from the same lead array can limit choices for therapy or recording. Further, beta band phenomena are strongly affected by normal voluntary movement³, which may complicate their use as signatures of motor impairment.

From invasive brain recordings, several neural signatures have been identified that may index the severity of parkinsonian motor signs or the presence of stimulation-induced adverse effects. Neural signatures may be detected in the motor cortex as well as the basal ganglia. Recently we characterized a distinctive narrowband gamma oscillation (60-90 Hz) detectable in human motor cortex, which occurs during dyskinesia⁴ (Figure 1A). This signature is associated with dyskinesia that occurs following medication alone and also dyskinesia which occur during DBS⁴. It is not strongly modulated by voluntary movement and is distinct from the canonical broadband gamma changes that occur in motor cortex during voluntary movement.^{5,6} Moreover, during DBS at typical frequencies (i.e.130-160 Hz), if dyskinesia is present, the narrowband gamma oscillation occurs reliably at half the stimulation frequency⁴, possibly because of neuronal entrainment (Figure 1A and 1C). Since this signature of dyskinesia is not disrupted by voluntary movement and occurs in a predictable frequency range, it is a promising control signal for adaptive DBS.

Here we demonstrate unilateral adaptive DBS in two PD patients, in which the stimulation lead is in STN while the control signal is sensed from a permanent subdural paddle lead implanted over ipsilateral motor cortex. Both leads are attached to Activa PC+S (Medtronic), an investigational implantable pulse generator (IPG) that allows chronic recording as well as stimulation. Since STN stimulation can exacerbate dyskinesia, we utilized the dyskinesia-related cortical narrowband gamma signal to reduce the amplitude of STN stimulation when the gamma oscillation exceeded a preset threshold. The algorithm was initially implemented on an external computer that received the brain data streamed in real-time and updated the patient's DBS settings noninvasively via radio telemetry. We subsequently uploaded the algorithm to the patient's internal pulse generator (IPG) to demonstrate totally embedded closed loop control (illustrated in relation to current "open loop control" in Figure 2).

Methods

Patients and device implantation

We tested adaptive stimulation in two male patients (65 and 61 years old) who were previously implanted with Activa PC+S as part of a chronic brain recording study^{4,7,8}, but continue to experience mild to moderate dyskinesia in spite of optimization of stimulation parameters by a movement disorders neurologist. The patients were diagnosed with PD 8 and 7 years ago (respectively) and were implanted with DBS 3 years (Patient 1) and 1 year 11 months (Patient 2) prior to participation in this study. At surgery, their baseline Unified Parkinson's Disease Rating Scale (UPDRS) scores on and off medications were: 14 and 30 (Patient 1) and 14 and 29 (Patient 2). Patient 2 was implanted with only unilateral DBS. Patient's clinical stimulation settings are listed in Table 1. This protocol was approved by the UCSF institutional review board (protocol # 13-10878) under a physician sponsored investigational device exemption (IDE # G120283). The study was registered at [ClinicalTrials.gov](https://clinicaltrials.gov) (NCT01934296). Informed consent was obtained under the Declaration of the Principles of Helsinki. Patient 1 and 2 in this study correspond to Patient 3 and 2 respectively in our previous publication⁴.

Surgical procedures for implantation of stimulation and sensing leads have been described previously^{4,7}. In brief, in addition to the quadripolar cylindrical STN lead (Medtronic model 3389) that delivers DBS therapy, we implanted a permanent quadripolar paddle-type lead (Medtronic model 3587A) in the subdural space over motor cortex. The cortical lead has 1 cm spacing between contacts and was only utilized for sensing, not stimulation. Both leads were attached to Activa PC+S (Medtronic), an IPG enabled to sense and store field potentials. Because Activa PC+S was only implanted unilaterally, adaptive DBS was delivered only on one side. On the contralateral hemisphere Patient 1 was implanted with a standard clinical IPG without sensing capability (Activa SC) attached to an STN lead. The stimulation delivered by the Activa SC was not altered during adaptive DBS.

Control algorithms for adaptive DBS

Activa PC+S, in conjunction with appropriate firmware and external devices, has two interfaces for prototyping and implementing closed loop DBS. The "Nexus D3" interface implements adaptive DBS using an external computer. Neural data are streamed to the external computer which implements the control algorithm and then updates stimulation.⁹ This approach is helpful for rapid algorithm prototyping and visualization of signals in real-time before implementing fully embedded adaptive DBS, for which algorithm troubleshooting is more challenging. The "Nexus E" interface allows for simple control algorithms, based on spectral power in pre-specified frequency bands, to be implemented within Activa PC+S¹⁰. In this mode, patients are not tethered to external systems. While there are some power requirements associated with running the detection algorithm on the IPG (Nexus E), the translational potential is very high since this is currently the only way that adaptive DBS can be feasibly delivered long-term. An open-loop DBS control session was also completed as a comparison to the adaptive DBS sessions. DBS setting used for adaptive stimulation are shown in Table 2 and details for each of the adaptive algorithms and open-loop session are provided below. In brief, both adaptive methods used the cortical

electrocorticographic (ECoG) signal over motor cortex in the gamma (60-90 Hz) range to detect whether dyskinesia was likely. If the signal was high (suggesting dyskinesia was likely) stimulation in the ipsilateral STN was reduced, and if it was low, stimulation was increased (Figure 1B and Figure 2B).

Behavioral assessments

Video recordings of all testing sessions were reviewed *post hoc* by a blinded movement disorders neurologist (SM). Patients were on medications during each session. Patients were also blinded to stimulation type (adaptive versus open-loop). For Patient 1, clinical rating scales were performed every 20 minutes using the upper body portions of the Unified Parkinson's Disease Rating Scale (UPDRS, items 20a-c, 21a-b, and 23a-25b) and the Unified Dyskinesia Rating scale (UDYS¹¹). To summarize these scores we summed the values for each scale (UPDRS and UDYS) and averaged them over time. We also asked the patient how he felt at each clinical rating session (i.e. every 20 minutes), specifically if there was any change to his subjective state. The timing of medication relative to testing is provided in Table 3. Patient 2 performed a short testing session (10 minutes) without administering formal rating scales. Video during the session was reviewed by the neurologist for overt clinical changes during continuous versus adaptive testing.

Energy calculation

All analyses were conducted in Matlab with custom scripts or eeglab¹². Total energy use was calculated based on the method proposed by Koss and colleagues¹³. Here total energy delivered is expressed as:

$$TEED_{1sec} = ((voltage^2 \times frequency \times pulse\ width) / impedance) \times 1sec$$

Here our voltage measure takes the average voltage over time which encompasses the integration of the stimulation current on a per pulse basis and derives the average energy delivered over the closed loop period. Total energy used for the adaptive DBS session was compared to total energy for an open-loop session of the same length of time where the voltage was maintained at the higher level used for adaptive DBS throughout the session. Spectral power near the primary frequency of the DBS artifact was recorded during all sessions, to verify appropriate changes in DBS amplitude.

Prototyping algorithms using Nexus D3

The Nexus D3 interface for closed loop control from an external computer was tested in one subject (Patient 1). A bipolar cortical signal sampled at 422 Hz was streamed from the implanted Acliva PC+S device to an external computer. To measure the neural signature of interest, power was extracted in the frequency domain from a window centered at 80 Hz (half the DBS stimulation frequency) with a 2.5 Hz bandwidth. Power in this window was averaged over 30 seconds. When the average crossed a specified threshold, stimulation voltage was adjusted (increased when the power was below the threshold, decreased when it was above, see Figure 1B). The threshold for triggering stimulation updates was set at 2.5 standard deviations above the calibration mean, which was calculated from power in the

same 80 Hz-centered window from a separate data set collected prior to the start of the adaptive DBS algorithm, during a time period when the patient was not dyskinetic. DBS parameters were selected to be as close to the patient's clinical settings as possible, while minimizing artifacts related to stimulation and Activa PC+S recordings. (For instance, constant current was not used for algorithm prototyping due to artifacts associated with this mode⁴.) Details are provided in Table 2. The stimulation frequency for the contralateral, non-sensing IPG (Activa SC), was changed to 160 Hz to match the Activa PC+S side, to avoid artifacts at additional frequencies in the brain recording, however it was not dynamically changed during adaptive DBS. The DBS voltage was adjusted on the Activa PC+S side between a therapeutic high value (3V) and a lower value (1V or 1.5V) value. Initially a low value of 1 V was used but was subsequently raised to 1.5 V for better entrainment of gamma band activity to the desired frequency of 80 Hz.

Embedded closed loop DBS using Nexus E

Fully internalized adaptive DBS using the Nexus E interface was tested in two patients. In this prototype, the signals to drive adaptive DBS were derived from electrocorticography (ECoG) power channels that record power directly from the Activa PC+S device (recordings were filtered using an analog filter prior to digitization). The narrowband gamma signal related to dyskinesia occurs at half the stimulation frequency, when dyskinesia is present (Figure 1A and 1C)⁴. Thus, for Patient 1 the power channel was centered at 80 Hz (± 2.5 Hz) (since his stimulation was delivered at 160 Hz) and for Patient 2 the power channel was centered at 65 Hz (± 2.5 Hz) (since his stimulation was delivered at 130 Hz). We also recorded a second power channel from the same recording electrodes, to record stimulation artifact and detect algorithm-triggered changes. This, in conjunction with verification from the log file, was used to derive voltage for the total energy used calculation. The power channel recording was set at a center frequency slightly off the actual stimulation frequency to avoid saturation of the power channels (140 Hz for Patient 1 and 150 Hz for Patient 2). Power values were acquired at a sampling rate of 5 Hz. We also recorded full time domain signals from motor cortex for visualization. These were sampled at 422 Hz for Patient 1 and at 800 Hz for Patient 2. Different sampling rates were used to accommodate different desired lengths of recording sessions and to minimize artifact caused by interactions between the sampling rates, stimulation frequency, and center frequencies of power channels⁴.

Stimulation voltage was decreased when the gamma signal rose above a threshold and was maintained at that level for at least 600 ms, and was increased when it fell below the same threshold for the same amount of time. This 600 ms parameter was selected to allow quick responses to changes in the feedback signal, while balancing the need to minimize false detections. The threshold was determined based on previously collected data both in and outside of clinic that occurred with and without dyskinesia. This data was used to select the frequency of interest and to properly train the support vector machine which was used to implement the algorithm. Voltage was changed between a therapeutic high value (3 V for Patient 1 and 5 V for Patient 2) and a low value (1 V for both patients), on the side implanted with Activa PC+S. The higher values were chosen to be similar to those used for therapeutic stimulation and the lower value was chosen to be as low as possible but still entrain the gamma signal⁴. Stimulation parameters used for adaptive DBS are shown in

Table 2. Voltage ramp times were 4 seconds for increasing DBS voltages and either 1 second (Patient 1) or 4 seconds (for Patient 2) for decreasing DBS voltages. We used slower ramp times for increases in voltage to avoid the sensation of stimulation-induced paresthesia. A quick ramp-down time was used to quickly reduce, or prevent the worsening of, dyskinesia.

Open-Loop Control

As a comparison to the adaptive DBS testing with Nexus E, we also performed an open-loop control test on a different day, where DBS voltage was held constant, for both patients (3 V for Patient 1 and 5 V for Patient 2). For each patient, the open-loop session was designed to be as similar to the adaptive DBS session as possible. Compared to the adaptive DBS testing, the open-loop testing lasted approximately the same amount of time, was at approximately the same time of day, and occurred after about the same amount of time relative to the last medication dose.

Results

We developed a novel adaptive DBS algorithm first by prototyping an externalized control system in one patient before testing a totally embedded control system in two patients. The algorithm used a cortical physiological signature sensitive to dyskinesia to update DBS voltage values – reducing voltages when gamma power was above a threshold (indicating dyskinesia was likely) and increasing voltages when gamma power was below a threshold (suggesting dyskinesia was less likely)⁴. These adaptive stimulation sessions were compared to an open-loop session where DBS was on at the same voltage continuously. Since the patient's clinical state was variable (presence or absence of dyskinesia, time since last medication dose) several sessions were performed with breaks in between to capture epochs where dyskinesia was present. Results for clinical efficacy and total energy used were calculated from the longest session containing dyskinesia for both Nexus D3 and Nexus E. The open-loop session analyzed was the session that best matched the Nexus sessions for time since last medication dose. This match was closer for the Nexus E session than for Nexus D3.

Clinical Efficacy

Clinical efficacy as determined by examination of video-recorded clinical ratings by a blinded neurologist are presented in Table 3 for Patient 1. This is based on a 62 minute session of closed loop DBS using Nexus D3 and a 30 minute session of Nexus E. The patient had similar bradykinesia and dyskinesia scores for all three sessions (Nexus D3, Nexus E, and open-loop), and this is true whether bilateral or unilateral scores are considered (Table 3). He never had tremor, so these scores were not included in the analysis.

Patient 2 did not have formal clinical ratings, but was included in the study to demonstrate technical capability of Aactiva PC+S for fully embedded adaptive stimulation in a second subject. The blinded neurologist reviewed video during both sessions and reported no overt clinical difference between adaptive DBS (Nexus E) and open-loop DBS. Both subjects denied any awareness of changes in stimulation settings during testing sessions.

Total energy savings

Adaptive DBS resulted in less total energy use compared to open-loop DBS. For sessions using adaptive DBS during dyskinesia the total energy saved was 38% for Patient 1 using Nexus D3, and 45% and 39% for Patients 1 and 2 respectively using Nexus E. An important consideration is that there is an additional 10% battery cost associated with sensing the electrophysiology data and running the Nexus E algorithm. Nevertheless, the energy saved surpassed the energy used. Use of Nexus D3 is associated with a more significant energy cost associated with streaming the data, which we did not consider for this study since the purpose of Nexus D3 was for prototyping our algorithms, not clinical application.

Algorithm performance

During the adaptive DBS session using the external adaptive DBS system (Nexus D3), 72 transitions (instances where the threshold was crossed) were triggered (over 64 minutes) for Patient 1 (Figure 3). For the same patient, 490 transitions were triggered (over 30.5 minutes) using the totally embedded system (Nexus E, Figure 4). For Patient 2, 158 transitions were triggered (over 10 minutes) using the embedded system (Nexus E). The zoomed in views of state changes in Figures 3c and 4b indicate that changes in classifier state were appropriately triggered by changes in gamma power.

Discussion

We have demonstrated the feasibility of adaptive DBS in PD using a fully implantable device, with feedback control provided by a cortical gamma band oscillation related to the emergence of dyskinesia, a common adverse effect of levodopa therapy and of STN DBS. While the total energy delivered by adaptive stimulation was substantially less than that of open-loop stimulation, blinded clinical ratings confirmed similar efficacy for both approaches. The classifier algorithm performed as expected, appropriately detecting changes in gamma band power and triggering reduction in DBS amplitude when the gamma threshold was exceeded. Adaptive DBS was tested in two modes of action: during data streaming from the implantable device to an external computer hosting the control algorithm, and with the control algorithm totally embedded within the pulse generator. Our goal was not to demonstrate clinical superiority of adaptive stimulation, but to perform short-term testing of a simple control algorithm as a foundation for a trial of adaptive DBS in a chronic, ambulatory setting.

Cortical versus basal ganglia control strategies

Prior published work on the use of neural control signals for adaptive DBS in PD has utilized STN LFPs recorded from the same DBS lead used for therapeutic stimulation. Although this approach has shown promise^{1,2}, the STN LFP is a low amplitude signal that is strongly affected by stimulation artifact when stimulation is delivered on adjacent contacts. Thus far, this approach has been tested largely with temporarily externalized STN leads, and may be difficult to translate into a fully implanted system given the less favorable signal to noise ratio characteristics, the larger stimulation artifact present in fully implanted systems compared to external recording systems⁷ and challenges of recording and stimulating from the same array. Indeed, for our particular control strategy (using a narrowband gamma

feedback signal), the signal was more reliably detected in cortex compared to STN both on and off DBS (Figure 5). Furthermore, as we showed in our previous paper, the cortical signal was associated with an area under the curve value of 0.912 from a receiver operator curve analysis, compared to a value of 0.797 for STN⁴. In contrast, our approach utilizes an ECoG signal for feedback control, provides a higher amplitude signal that is much further from the source of stimulation artifact and does not limit the choice of DBS contacts available for stimulation (given the inability to record and stimulate from the same contact). This last point bears particular consideration since often the contacts in STN which best detect signatures related to symptoms are also the contacts which correspond to the regions of STN most likely to be targeted for clinical use¹⁴. We have demonstrated the technical feasibility of this approach within a totally implanted device. While this cortical detection strategy does require insertion of a subdural lead for motor cortex recording, insertion of this “extra” lead is technically simple and can be done at the same time as insertion of the DBS leads, using the same skull opening and surgical exposure as used for the DBS leads⁷. Additionally, the insertion of this lead has not been associated with negative outcomes when used acutely¹⁵ or chronically (in a small sample)⁷.

Neural control utilizing STN signals has focused on beta band oscillations, a possible marker of the severity of parkinsonism whose amplitude is reduced by therapeutic DBS and dopaminergic medication^{16,17}. A challenge to using a beta-derived control signal is that it is strongly modulated by normal behaviors including voluntary movement³. For adaptive DBS in the chronic ambulatory setting, the control algorithm would have to distinguish between beta changes related to bradykinesia and those related to voluntary movement. This is less of a concern for the cortical control strategy demonstrated here, since feedback control utilized a narrowband gamma oscillation which is not strongly modulated by voluntary movement⁴. Of note, this narrowband gamma oscillation is larger than, and distinct from, the low amplitude, broadband gamma signal detectable in ECoG recordings that is modulated by normal movement and probably reflects asynchronous (non-oscillatory) processes^{5,6}.

Is adaptive DBS necessary?

Standard, open-loop continuous DBS has been shown to be highly effective for PD in randomized clinical trials¹⁸. However, there are several reasons why adaptive DBS could improve this therapy. Reduction in stimulation current without loss of therapeutic benefit has the potential to reduce stimulation-induced adverse effects¹⁹, as well as prolong battery life or allow greater miniaturization of the relatively large pulse generators now in use²⁰. Further, some of the PD patients most in need of DBS are also among the most difficult to successfully program: those who alternate between extreme states of dyskinesia and bradykinesia with little in-between time (“brittle fluctuators”)^{21,22}. Previous research has estimated the percentage of patients who exhibit this “brittle” pattern is between 2-6%^{21,22}. Although the percentage is relatively low, there is a high need for a solution for these patients as their dyskinesia tends to be more severe and more painful and they can be extremely sensitive to stimulation-induced dyskinesia²¹. Furthermore the lessons learned from this approach may have broader implications. For instance, as a therapeutic strategy for other disorders associated with hyperkinetic movements following DBS²³.

While for some patients simply manually adjusting their own DBS settings might be sufficient to avoid frequent dyskinesia, for others, especially patients with very frequent motor fluctuations, such an approach would be cumbersome and imprecise. Additionally, many patients have co-morbid cognitive impairment, which would preclude active monitoring of their clinical state and devices. Thus an adaptive algorithm that automatically titrated stimulation to avoid dyskinesia could be useful. Motor fluctuations in patients in this pilot study were less extreme, which may explain why adaptive DBS in this short-term study did not show therapeutic superiority over open-loop continuous DBS. Indeed, it is possible there could have been a floor effect for dyskinesia in this study since dyskinesia was mild for all conditions (see Table 3). Another possibility is that bilateral adaptive stimulation may be necessary for clinical benefit and that this is why we did not see a clinical improvement (since we tested only unilateral adaptive DBS). Of note, adaptive DBS using neural control embedded within a totally implantable device has shown promise in other movement disorders, including Tourette's syndrome²⁴ and essential tremor²⁵.

Another consideration is that our results apply specifically to STN DBS, which is currently the most commonly used target for DBS in PD. An alternative surgical target for DBS is the globus pallidus interna (GPi). GPi DBS is less associated with dyskinesia postoperatively and, therefore, a dyskinesia-based control strategy may not be as useful for these patients. However, there are disadvantages to GPi DBS including a shorter battery life and diminished ability to lower medication dosages postoperatively²⁶.

Limitations

Here, we utilized a simple single threshold control strategy with a sensitive detector that allowed us to demonstrate technical success of adaptive stimulation during brief, in-clinic testing. Using this approach transitions in the classifier state occurred much more frequently than would be expected if transitions were only triggered by changes in the clinical state of the patient. Rather, multiple transitions were triggered by relatively small fluctuations in the neural signal, fluctuations which were likely too small to correlate with overt behavioral changes. A sensitive algorithm was desired for this brief in-clinic test to ensure that the system was accurately detecting changes in the neural signals and adjusting stimulation accordingly. Further, the amplitude of the neural signal used for control (gamma band power) also fluctuated rather than stabilized, possibly in part due to frequent voltage transitions.

One way to dampen rapid changes in stimulation, in the setting of a sensitive classifier, is to utilize a slow ramp for stimulation voltage changes when the classifier detects change. The ramp times utilized here were between 1-4 seconds. Because of this, while many transitions were triggered, DBS voltages did not change as often since the voltage was set to ramp slowly (Figure 3b). Even longer ramp times could be used to achieve even more stable voltages. Other alternatives, especially for longer-term testing, is to increase the threshold for triggering a change in DBS, or to use a two-threshold control strategy. These modifications might result in fewer transitions, greater stability in the neural signature of dyskinesia, and closer tracking of the clinical state of the patient. With two thresholds, the classifier would change to the "reduced gamma" state after the control signal declined below

the lower threshold, but would not change back to the “elevated gamma” state until the control signal rose above the higher threshold. Of note, at this time using the fully embedded (Nexus E) Aactiva PC+S strategy, only single level control is possible.

It should be noted that rapid transitions in classifier state are not necessarily detrimental. Adaptive control algorithms utilizing STN beta band oscillations also showed rapid transitions in the classifier with frequent fluctuations in DBS amplitude¹, but these fluctuations nevertheless served to “shape” the neural signal in a therapeutically useful way, by shortening the duration of “bursts” of beta activity²⁷.

Finally, we did not specifically compare adaptive stimulation based on neural feedback to intermittent open-loop stimulation since the goal of the study was to show technical feasibility of adaptive DBS in a short-term trial.

Conclusions

We have demonstrated the feasibility of adaptive DBS using a cortical detector sensitive to dyskinesia in two patients. In both patients there were energy savings without worsening of clinical symptoms. This strategy requires further testing in a chronic ambulatory setting, and may be useful in PD patients who are motor fluctuators and experience severe dyskinesia alternating with marked bradykinesia^{21,22}. This work illustrates a systematic approach to algorithm development in a neural interface, beginning with the use of sensing for biomarker discovery, then in-clinic testing using an external computer for flexibility in algorithm development, and finally use of control algorithm that is totally embedded within the device.

Acknowledgments

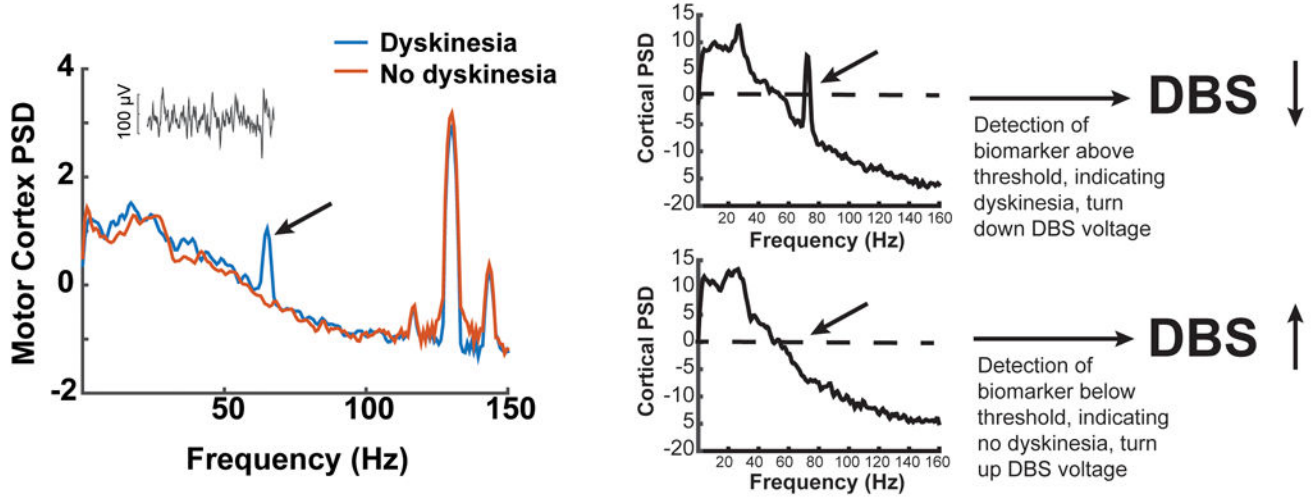
This project was supported by NIH grants (NS090913-01 and NS100544-02) and the UC President’s Postdoctoral Fellowship. We thank Maryam Shanechi and Simon Little for their critical review of the manuscript and Witney Chen, Preeya Khanna, and Shelia Rajagopalan for their help with data collection. Engineers at Medtronic, Inc. reviewed the manuscript for technical accuracy.

References

1. Little S, Pogosyan A, Neal S, et al. Adaptive deep brain stimulation in advanced Parkinson disease. *Annals of neurology*. 2013; 74(3):449–457. [PubMed: 23852650]
2. Rosa M, Arlotti M, Ardolino G, et al. Adaptive deep brain stimulation in a freely moving Parkinsonian patient. *Mov Disord*. 2015; 30(7):1003–1005. [PubMed: 25999288]
3. Kuhn AA, Williams D, Kupsch A, et al. Event-related beta desynchronization in human subthalamic nucleus correlates with motor performance. *Brain*. 2004; 127(Pt 4):735–746. [PubMed: 14960502]
4. Swann NC, de Hemptinne C, Miocinovic S, et al. Gamma Oscillations in the Hyperkinetic State Detected with Chronic Human Brain Recordings in Parkinson’s Disease. *J Neurosci*. 2016; 36(24):6445–6458. [PubMed: 27307233]
5. Crone NE, Miglioretti DL, Gordon B, Lesser RP. Functional mapping of human sensorimotor cortex with electrocorticographic spectral analysis. II. Event-related synchronization in the gamma band. *Brain*. 1998; 121(Pt 12):2301–2315. [PubMed: 9874481]
6. Miller KJ, Leuthardt EC, Schalk G, et al. Spectral Changes in Cortical Surface Potentials during Motor Movement. *Journal of Neuroscience*. 2007; 27(9):2424–2432. [PubMed: 17329441]
7. Swann NC, de Hemptinne C, Miocinovic S, et al. Chronic multisite brain recording from a totally implantable bidirectional neural interface: experience in five patients with Parkinson’s disease. *Journal of neurosurgery*. 2017 in press.

8. Khanna P, Swann N, De Hemptinne C, et al. Neurofeedback Control in Parkinsonian Patients Using Electrocortigraphy Signals Accessed Wirelessly With a Chronic, Fully Implanted Device. *IEEE Trans Neural Syst Rehabil Eng.* 2016
9. Herron J, Chizeck HJ. Prototype closed-loop deep brain stimulation systems inspired by Norbert Wiener. *IEEE Conference on Norbert Wiener in the 21st Century.* 2014
10. Afshar P, Khambhati A, Stanslaski S, et al. A translational platform for prototyping closed-loop neuromodulation systems. *Front Neural Circuits.* 2012; 6:117. [PubMed: 23346048]
11. Goetz CG, Nutt JG, Stebbins GT. The Unified Dyskinesia Rating Scale: presentation and clinimetric profile. *Mov Disord.* 2008; 23(16):2398–2403. [PubMed: 19025759]
12. Delorme A, Makeig S. EEGLAB: an open source toolbox for analysis of single-trial EEG dynamics including independent component analysis. *Journal of neuroscience methods.* 2004; 134(1):9–21. [PubMed: 15102499]
13. Koss AM, Alterman RL, Tagliati M, Shils JL. Calculating total electrical energy delivered by deep brain stimulation systems. *Annals of neurology.* 2005; 58(1):168. author reply 168–169. [PubMed: 15984018]
14. Trottenberg T, Kupsch A, Schneider GH, Brown P, Kuhn AA. Frequency-dependent distribution of local field potential activity within the subthalamic nucleus in Parkinson's disease. *Experimental neurology.* 2007; 205(1):287–291. [PubMed: 17336961]
15. Panov F, Levin E, de Hemptinne C, et al. Intraoperative electrocortigraphy for physiological research in movement disorders: principals and experience in 200 cases. *Journal of neurosurgery.* 2016 in press.
16. Kühn AA, Kempf F, Brücke C, et al. High-frequency stimulation of the subthalamic nucleus suppresses oscillatory beta activity in patients with Parkinson's disease in parallel with improvement in motor performance. *J Neurosci.* 2008; 28(24):6165–6173. [PubMed: 18550758]
17. Kühn AA, Kupsch A, Schneider G-H, Brown P. Reduction in subthalamic 8–35 Hz oscillatory activity correlates with clinical improvement in Parkinson's disease. *Eur J Neurosci.* 2006; 23(7): 1956–1960. [PubMed: 16623853]
18. Deuschl G, Schade-Brittinger C, Krack P, et al. A randomized trial of deep-brain stimulation for Parkinson's disease. *The New England journal of medicine.* 2006; 355(9):896–908. [PubMed: 16943402]
19. Little S, Tripoliti E, Beudel M, et al. Adaptive deep brain stimulation for Parkinson's disease demonstrates reduced speech side effects compared to conventional stimulation in the acute setting. *Journal of neurology, neurosurgery, and psychiatry.* 2016; 87(12):1388–1389.
20. Meidahl AC, Tinkhauser G, Herz DM, Cagnan H, Debarros J, Brown P. Adaptive Deep Brain Stimulation for Movement Disorders: The Long Road to Clinical Therapy. *Mov Disord.* 2017; 32(6):810–819. [PubMed: 28597557]
21. Martinez-Ramirez D, Giugni J, Vedam-Mai V, et al. The “brittle response” to Parkinson's disease medications: characterization and response to deep brain stimulation. *PLoS One.* 2014; 9(4):e94856. [PubMed: 24733172]
22. Sriram A, Foote KD, Oyama G, Kwak J, Zeilman PR, Okun MS. Brittle Dyskinesia Following STN but not GPi Deep Brain Stimulation. *Tremor Other Hyperkinet Mov (N Y).* 2014; 4:242. [PubMed: 24932426]
23. Ostrem JL, Racine CA, Glass GA, et al. Subthalamic nucleus deep brain stimulation in primary cervical dystonia. *Neurology.* 2011; 76(10):870–878. [PubMed: 21383323]
24. Shute JB, Okun MS, Opri E, et al. Thalamocortical network activity enables chronic tic detection in humans with Tourette syndrome. *NeuroImage Clinical.* 2016; 12:165–172. [PubMed: 27419067]
25. Herron J, Thompson M, Brown T, Chizeck H, Ojemann J, Ko A. Cortical brain computer interface for closed-loop deep brain stimulation. *IEEE Trans Neural Syst Rehabil Eng.* 2017
26. Williams NR, Foote KD, Okun MS. STN vs. GPi Deep Brain Stimulation: Translating the Rematch into Clinical Practice. *Mov Disord Clin Pract.* 2014; 1(1):24–35. [PubMed: 24779023]
27. Tinkhauser G, Pogosyan A, Little S, et al. The modulatory effect of adaptive deep brain stimulation on beta bursts in Parkinson's disease. *Brain.* 2017; 140(4):1053–1067. [PubMed: 28334851]

A. Biomarker related to dyskinesia B. Schematic of closed loop DBS



C. Shifting peak frequency during dyskinesia based on DBS frequency



Figure 1.

A. Example of power spectral densities from motor cortex recorded with and without dyskinesia, both during DBS. Inset shows raw motor cortex signal when DBS was off. Black arrow indicates narrowband gamma signal used for feedback (adapted from Swann et al. 2016). B. Schematic of closed loop algorithm. DBS voltage is decreased if narrowband gamma exceeds a threshold and increased when below the threshold. C. Example of the change in the peak frequency of the narrowband gamma with DBS. DBS caused the frequency to shift to half the stimulation frequency (adapted from Swann et. al 2016).

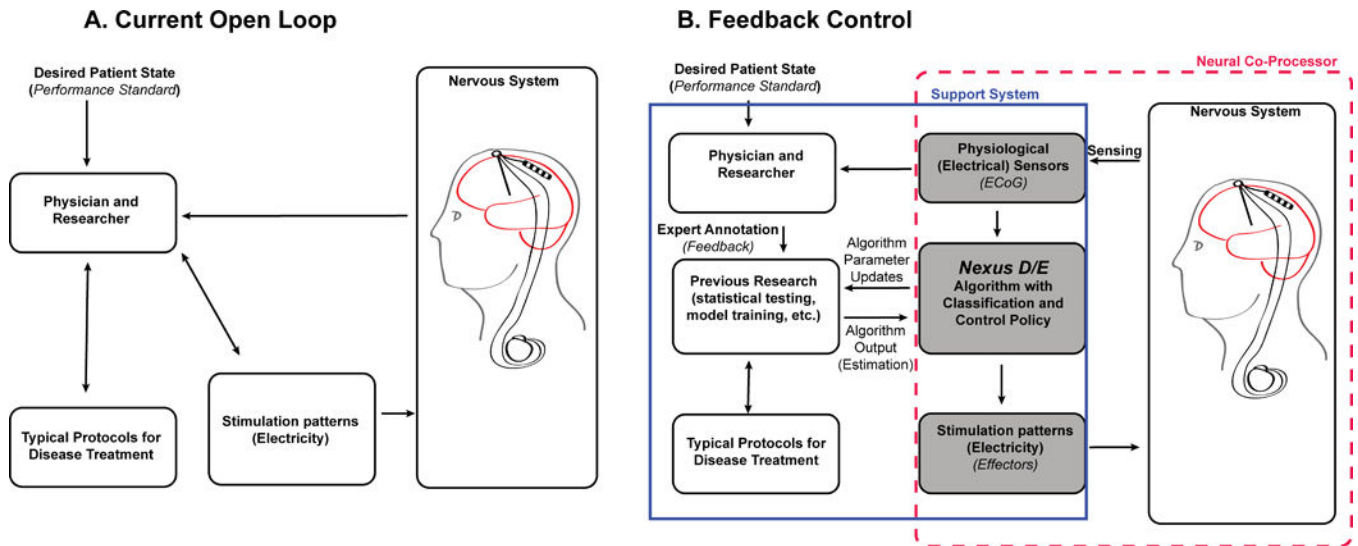


Figure 2. Schematics of current Open Loop (A) and Feedback Controlled (B) DBS. Note that in the Feedback Controlled version (B) the portion labeled “Nexus D/E” is external in the case of Nexus D and internal for Nexus E.

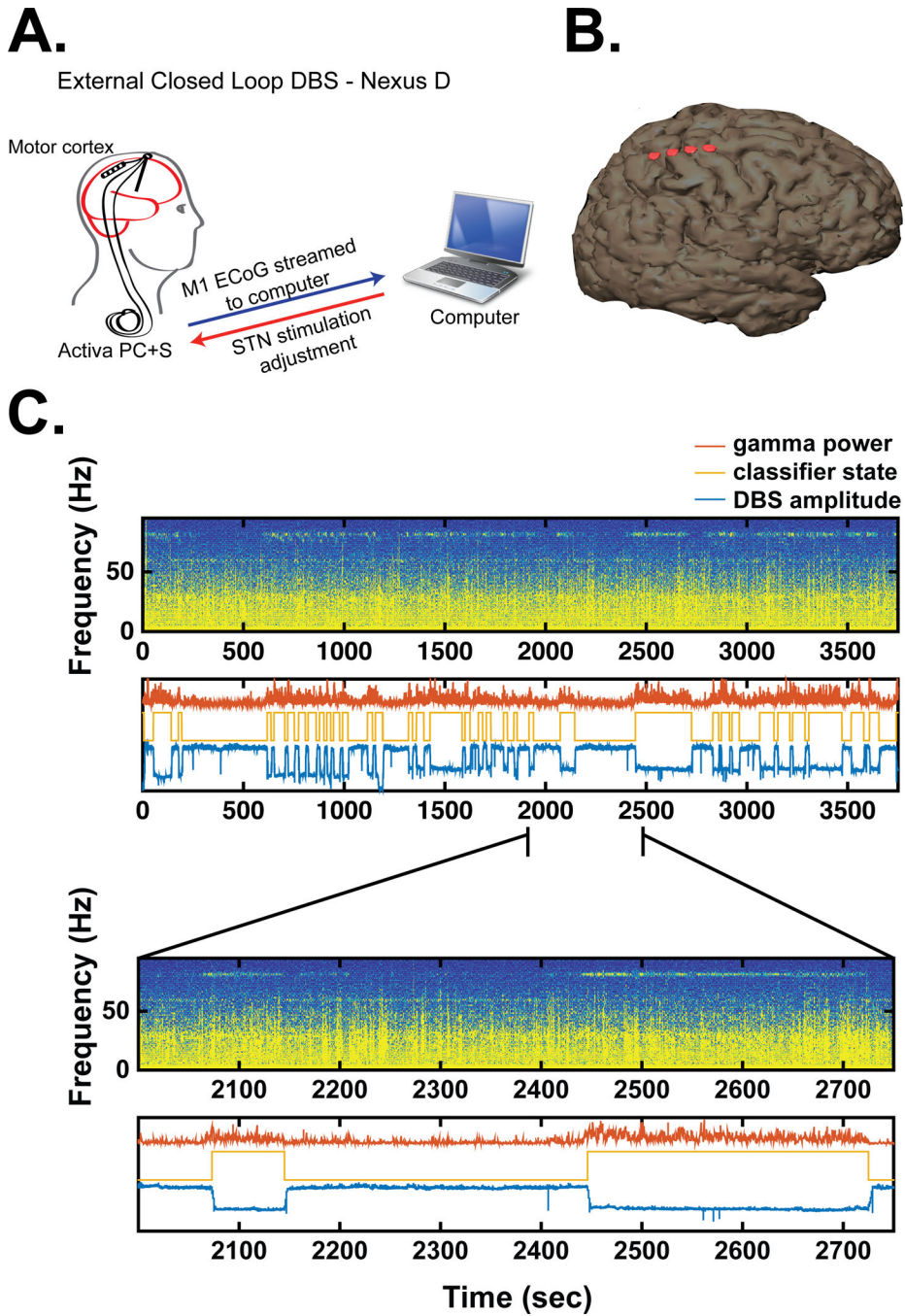
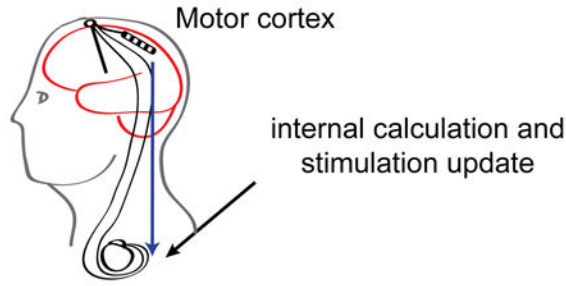


Figure 3. Adaptive DBS utilizing Activa PC+S under control of an external computer (Nexus D3), from patient 1. **A.** Schematic illustration of external control. **B.** 3-D reconstruction of patient’s brain and ECoG contacts used for sensing, derived from postoperative CT images computationally fused to a preoperative brain MRI. **C.** Neural data, classifier state, and stimulation state during adaptive DBS. Top panel: Spectrogram of time domain signal recorded from motor cortex for longest adaptive DBS session during which dyskinesia occurred. Second panel: classifier state (gold), DBS voltage (blue), and gamma power used

as the control signal (red). The y-axis is in arbitrary units. Lower panels show a zoomed in view to demonstrate that classifier state transitions correspond appropriately to fluctuations in gamma band power.

A. Embedded Closed Loop DBS - Nexus E



B. Activa PC+S

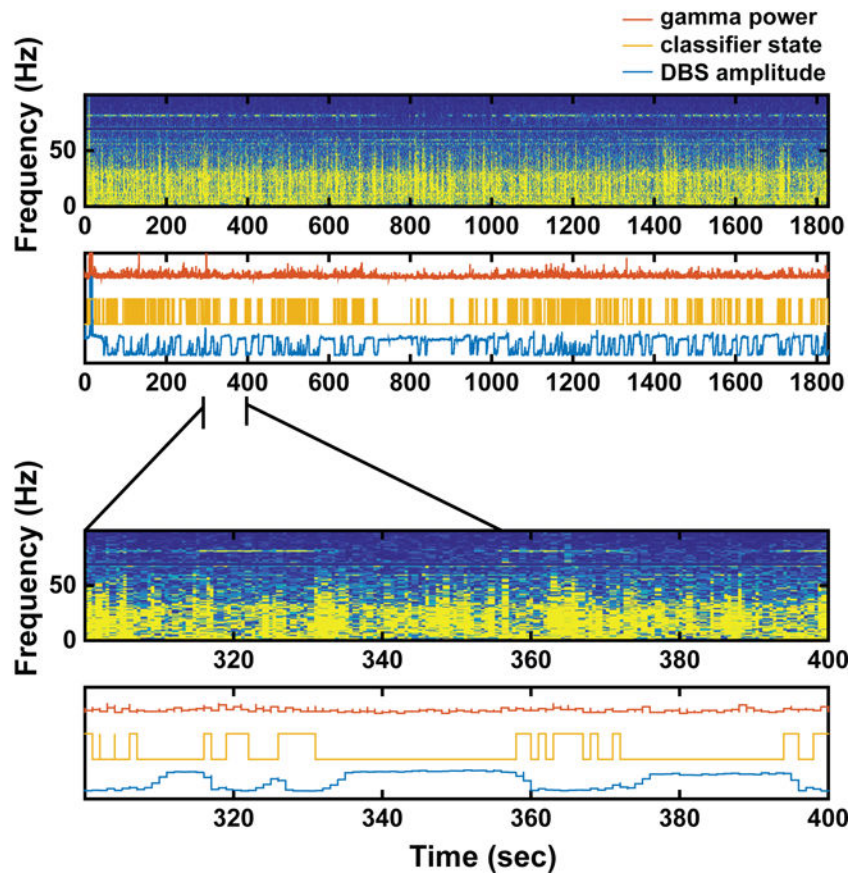


Figure 4. Adaptive DBS utilizing Activa PC+S with fully embedded control (Nexus E), from Patient 1. A. Schematic of fully embedded control. B. Neural data, classifier state, and stimulation state during adaptive DBS. Panel format same as Figure 2. Note the more frequent transitions in the classifier compared to Nexus D3. This is likely because the Nexus E algorithm did not incorporate any smoothing of the signal, whereas Nexus D3 averaged the gamma signal over time before triggering a change in stimulation. This type of smoothing was not supported by Nexus E.

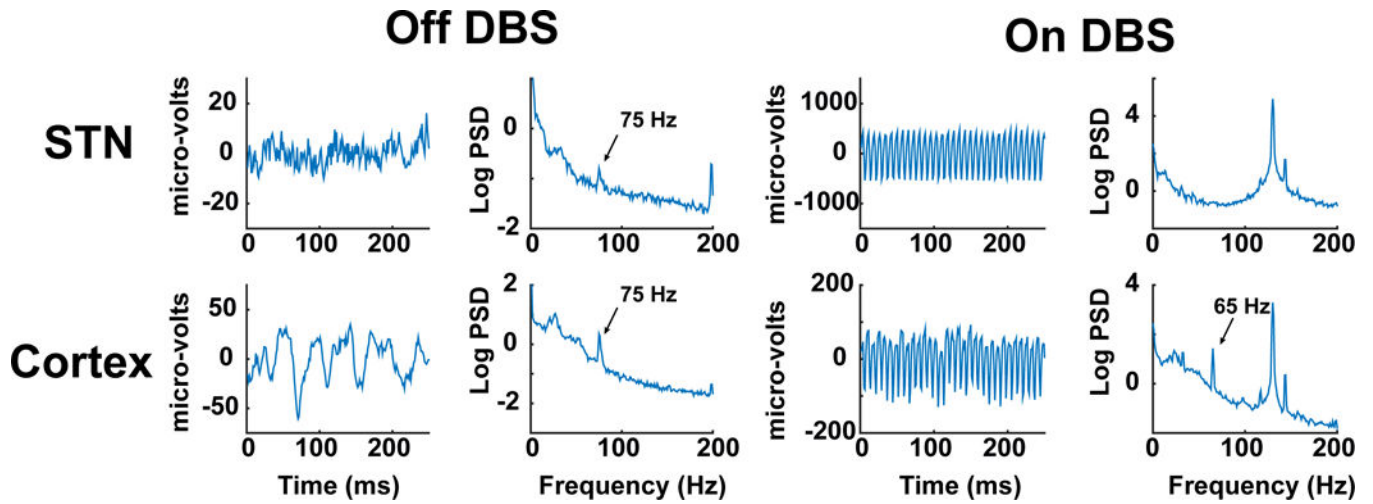


Figure 5.

Examples of time series of the STN LFP and M1 ECoG potential, and their power spectra, both on and off DBS. The gamma peak in the power spectrum is larger for cortical recordings. There is prominent stimulation artifact for both recording sites with DBS on. While the gamma peak in the power spectrum of the STN LFP is totally obscured during DBS on, the M1 gamma peak remains detectable, underscoring the utility of the M1 signal for feedback control. Note the differing scales of the y-axis for STN versus M1.

Table 1

Stimulation parameters used for standard clinical DBS, prior to starting this study. Patient 2 has unilateral DBS.

Patient #	Activa PC+S (stimulation and sensing)				Activa SC (stimulation, no sensing)					
	Brain Side	Active Contacts ^a	Amplitude	Pulse Width (µsec)	Frequency (Hz)	Brain side	Active Contacts	Amplitude	Pulse Width (µsec)	Frequency (Hz)
1	R	C+1-	3V	60	150	L	C+3-	5.2 mA	60	130
2	L	C+2-	5.4 mA	90	130	N/A	N/A	N/A	N/A	N/A

^a AC-PC coordinates of the active contacts, expressed as lateral (x), anterior (y), and superior (z) distances from the midcommissural point, were -10.59, -2.61, -2.06 (x,y,z, patient 1) and -13.78, 4.74, -2.10 (x,y,z, patient 2).

Table 2

Stimulation parameters of the Activa PC+S device during adaptive DBS.

Patient #	Brain Side	Active stimulation Contacts	AC-PC coordinates of ECoG recording contact pairs ^a			Amplitude range for adaptive (V)	Pulse Width (µsec)	Amplitude for continuous (V)	Frequency (Hz)
			x	y	z				
1	R	C+1-	29.23	-17.86	66.22	1 ^b -3	60	3	160
			30.40	-7.63	65.36				
2	L	C+2-	28.43	-14.90	67.61	1-5	90	5	130
			28.43	5.02	63.59				

^aCoordinates are expressed as the lateral (x), anterior (y), and superior (z) distances from the midcommissural point. Note that two sets of coordinates are provided because each ECoG signal was recorded from a pair of electrodes that were bipolar referenced.

^bNote, part-way through the Nexus D3 run the lower limit was adjusted to 1.5 V. The lower limit was still 1 V for Nexus E.

Table 3

Clinical Ratings from Patient 1. Bradykinesia score is derived from items 23a-25b of the UPDRS and Dyskinesia score is derived from the UDYS rating scale. In both cases, scores were summed and then averaged across time. We have reported rating scales which are both bilateral and unilateral (reflecting the side of the body contralateral to the side modulated by adaptive DBS.) Note that for the dyskinesia rating scale the highest theoretical score is 28, so patient's overall dyskinesia was relatively low, suggesting that a floor effect could be occurring.

Stimulation mode	Bradykinesia Score Total/Contralateral only	Dyskinesia Score Total/Contralateral only	Total Energy Saved Relative to Open-loop	Minutes Since Last Medication Dose (session start-session end)
Adaptive, Nexus D3	14/7	1.5/1.25	38%	110-175
Adaptive, Nexus E	11.83/4.67	1.33/1.33	45%	65-110
Open-loop	12.33/5.67	1.667/1.33	0%	70-110